International Journal of Engineering, Mathematical and Physical Sciences
ISSN: 2517-9934
Vol:4, No:5, 2010

Bifurcation Analysis of Horizontal Platform System

C. C. Wang, N. S. Pai, H. T. Yau, T. T. Liao, M. J. Jang, C. W. Lee and W. M. Hong

***Abstract*—**Horizontal platform system (HPS) is popularly applied in offshore and earthquake technology, but it is difficult and time-consuming for regulation. In order to understand the nonlinear dynamic behavior of HPS and reduce the cost when using it, this paper employs differential transformation method to study the bifurcation behavior of HPS. The numerical results reveal a complex dynamic behavior comprising periodic, sub-harmonic, and chaotic responses. Furthermore, the results reveal the changes which take place in the dynamic behavior of the HPS as the external torque is increased. Therefore, the proposed method provides an effective means of gaining insights into the nonlinear dynamics of horizontal platform system.

***Keywords*—**horizontal platform system, differential transformation method, chaotic.

I. Introduction

IN the past two decades, people are naturally interested in the dynamic is the basis of chaotic system, such as highly complex dynamics, broad-band Fourier power spectrums and strong attractors [1], [2]. We can know that by the references, the theoretical analysis and the experiment is the synchronization problems; they will be effectively solved and performed [3]-[5]. On the other hand, in the years the several mechanical systems of chaos phenomenon were to observe [6], [7]. In the mechanical systems the HPS behaves chaotic motion at specific conditions, and can be free to rotate round along horizontal axis, therefore HPS was used widely in offshore and earthquake technology research [8]. In the HPS systems the chaos synchronization problems was proposed and solved [9]. A novel feedback controller was designed for synchronization between master-slaves HPS [10]. Also, a robust synchronization of HPS with phase differences was presented [11].

The aim of this paper is to demonstrate the bifurcation of HPS under different external torques parameter and understand the dynamic behaviors of the HPS. In order to analyze the HPS, the differential transformation method is used and compared with Runge-Kutta method. Furthermore, we confirm whether the HPS is periodic or chaos phenomenon applying phase portraits, power spectra, Bifurcation diagrams, Poincaré maps and Lyapunov exponents.

The remainder of this study is organized as follows. Section 2 is dynamics equation and differential transformation method. The simulation and experimental results are shown in Section3. Finally, Section 4 draws some brief conclusions.

C. C. Wang is with the Far East University, Tainan, Taiwan (corresponding author to provide phone: 886-6-5979566; fax: 886-6-5977115; e-mail: wccpipn@gmail.com).
N. S. Pai, is with the National Chin-Yi University of Technology, Taichung County 411, Taiwan (e-mail: pai@mail.ncut.edu.tw).
H. T. Yau, is with the National Chin-Yi University of Technology, Taichung County 411, Taiwan (e-mail: htyau@mail.ncut.edu.tw).
T. T. Liao is with the Far East University, Tainan, Taiwan (e-mail: ttliao@cc.feu.edu.tw).
M. J. Jang is the vice President of Far East University, Tainan, Taiwan (e-mail: mjjang@cc.feu.edu.tw).
C. W. Lee, is with the Far East University, Tainan, Taiwan (e-mail: yuwnn@hotmail.com).

II. Mathematical Modeling

A. Equation of Motion for HPS

The HPS is shown in Fig.1. The horizontal platform rotates around the horizontal axis, which perforates into its mass center. There is an accelerometer located on the platform to measure the position. When the platform varies from horizon, the accelerometer will produce a signal to the actuator that provides a reverse torque to balance the rotation of HPS. The equation of the system is:

$$C_1\ddot{x}(t)+C_d\dot{x}(t)+gC_a\sin x(t)-\frac{3g}{R_e}(C_2-C_3)\cos x(t)\sin x(t) = F\cos\omega t \quad (1)$$

where C_1, C_2 and C_3 are the inertia moment of the platform for axis 1, 2 and 3, respectively. C_d is the damping coefficient, R_e is the radius of the earth, C_a is the proportional constant of the accelerometer, the g is the constant of gravity, and x is the rotation of the platform relative to the earth. $F\cos\omega t$ indicates the external torque. This system details analysis was show in [12]. The $x_1(t)=x(t)$ and $x_2(t)=\dot{x}(t)$ are denoted the state variables. The HPS model (1) can be rewritten as follows：

$$\dot{x}_1(t)=x_2(t) \quad (2)$$

$$\dot{x}_2(t)=-\frac{C_d}{C_1}x_2(t)+\frac{3g}{C_1R_e}(C_2-C_3)\cos x_1(t)\sin x_1(t) - g\frac{C_a}{C_1}\sin x_1(t)+\frac{F}{C_1}\cos\omega t \quad (3)$$

B. Differential Transformation Method

Differential transformation is one of the most widely used of all techniques for solving differential equations due to its rapid rate of convergence and its minimal computational error. Furthermore, compared to the integral transformation approach, differential transformation has the further advantage that it can be used to solve nonlinear differential equations. In

solving (2), and (3) using the differential transformation method, the HPS model is transformed with respect to the time domain, and hence the equation becomes[13]-[15]

$$\frac{k+1}{H}\bar{X}_1(k+1)=\bar{X}_2(k) \tag{4}$$

$$\frac{k+1}{H}\bar{X}_2(k+1)=-\frac{C_d}{C_1}\bar{X}_2(k)+\frac{3g}{C_1R_e}(C_2-C_3)cos\bar{X}_1\otimes sin\bar{X}_1 - g\frac{C_a}{C_1}sin\bar{X}_1+\frac{F}{C_1}\frac{(\omega H)^k}{k!}cos\left(\frac{\pi k}{2}\right) \tag{5}$$

III. Results and Discussions

A. Numerical Simulation Results

As discussed above, the nonlinear behavior of the HPS is analyzed in this study using the differential transformation method (DTM). The dynamic behavior of the horizontal platform system is characterized by reference to power spectra, Poincaré maps, maximum Lyapunov exponent plots and bifurcation diagrams produced using the time-series data for the displacement and velocity of the center of gravity. Note that in producing these various plots, the time-series data corresponding to the first 1000 revolutions are deliberately excluded in order to ensure that the results reflect steady-state conditions.

Table 1 compares the results obtained by the DTM and the Runge-Kutta method (RKM) for the relative rotation of the platform at various values of *F*. It is seen that a good agreement exists between the two sets of numerical results. It also clarifies the effect of the time-step value on the Poincaré maps for the center of gravity at different values of *F*. It can be seen that for a given *F*, the rotation calculated using different values of the time step are in agreement to approximately 4~5 decimal places for DTM.

B. Phase Portraits

As shown in Fig.2, the phase portraits of the HPS at various values of the torque *F*, are regular and symmetrical, i.e. the center exhibits a periodic response. Figs. 2(a)~2(h) reveal that the orbit is regular at low value of *F*= 1.33, but becomes irregular when the *F* is increased to 2.78. When *F* is increased further to 3.21, the orbit performs from regular to non-periodic motion. Finally, the HPS transfers to periodic motion at *F* =3.59.

C. Power Spectra

Fig. 3 shows the power spectra of the HPS responses. At *F* =1.33, the power spectra show that the HPS performs 5T-periodic motion. However, when *F* is increased to 3.59, it can be seen that the HPS exhibits multi-periodic motion. At *F*=2.78 and 3.21, the system has a chaotic behavior.

D. Maximum Lyapunov Exponents

The maximum Lyapunov exponent can also be used to identify the dynamic behavior of the HPS. Figs. 4(a) and 4(d), corresponding to *F*=1.33, 3.59, respectively, show that the maximum Lyapunov exponent has a value of approximately zero, which indicates that the system has a periodic response. However, at *F*=2.78 and 3.21, shown in Figs. 4(b) and 4(c), respectively, the maximum Lyapunov exponent is positive, and hence it can be inferred that the system has a chaotic response.

E. Bifurcation Diagrams and Poincaré Maps

In general, bifurcation diagrams and Poincaré maps summarize the essential dynamics of a system, and are therefore useful tools for observing nonlinear dynamic behavior. In the current study, Figs. 5(a) and 5(b) plot the bifurcation diagrams of the HPS over the interval $1.0\leq F \leq 10.0$, taking *F* as the bifurcation parameter. Figs. 5(c) and 5(d) plot the local bifurcation diagrams of the HPS over the interval $2.0\leq F \leq 4.0$. Finally, Figs. 6(a)-6(d) present the Poincaré maps of the HPS at *F*=1.33, 2.78, 3.21, and 3.59, respectively.

Fig. 5(c) and 5(d) show that at lower values of *F*, i.e. $F<2.78$, the HPS exhibits a dynamic periodic response, including 5T-, 10T- and multi-periodic motions. Fig. 6(a) presents the Poincaré map corresponding to $F=1.33$ and the map has five discrete points which confirms the existence of 5T-periodic behavior shown in the bifurcation diagrams. As the value of *F* is increased over the interval $2.78\leq F <2.95$, Fig. 5 and 6(b) show that HPS performs chaotic-periodic motion.

When *F* is increased over the interval $2.95\leq F <3.59$, the HPS response is sub-harmonic motion. Fig. 6(b) and Fig. 6(c) present the Poincaré maps at $F=2.78$ and 3.21, respectively and behave chaotic motion. The presence of chaos is observed at five intervals and shown in Table 2. As *F* is increased over the interval $3.59\leq F <3.61$, the HPS exhibits 10T-periodic motion, as shown in Fig. 6(d).

From the discussions above, it is clear that the dynamic response of the HPS depends on the magnitude of *F*. The various motions performed by HPS as *F* increases from 1.0 to 10.0 are summarized in Table 2. In general, the results show that depending on the value of *F*, the HPS may exhibit periodic behavior, i.e. 5T-, 10T- or multi-periodic motion, or a chaotic response. This result also indicates that a discontinuous increase takes place in the size and form of the chaotic attractor as *F* is increased.

IV. Conclusion

In the present paper the HPS has been studied and applied the differential transformation method and the Runge-Kutta method, respectively, to investigate the dynamic behavior of horizontal platform. Dynamic orbits, Poincaré maps, maximum Lyapunov exponent plots, and bifurcation diagrams have been used to characterize the dynamic response of the HPS as a function of the torque and to detect the occurrence of chaotic motion. In general, the results have shown that as the torque is increased from 1.0 to 10.0, the HPS behaves different kinds of dynamic responses including 5T-, 10T-, multi-periodic, and chaotic motions. In some intervals of torque, the HPS motion changes initially from 5T-periodic to 10T-periodic, and then from 10T-periodic to multi-periodic, and finally to chaotic motions.

ACKNOWLEDGMENT

This work is funded by The National Science Council (grant number NSC-98-2221-E-269-016, NSC-98-2221-E-269-012, NSC-98-2221-E-269-015).

REFERENCES

[1] A. N. Miliou, I. P. Antoniades, S. G. Stavrinides, and A. N. Anagnostopoulos,"Secure communication by chaotic synchronization: robustness under noisy conditions," *Nonlinear Analysis-Real World Applications*, vol. 8, pp. 1003-1012,July 2007.

[2] M. Chen, and W. Min,"Unknown input observer based chaotic secure communication," *Physics Letters A*, vol. 372, pp. 1595-1600, March 2008.

[3] C. K. Huang, S. C. Tsay, and Y. R. Wu,"Implementation of chaotic secure communication systems based on OPA circuits," *Chaos Solitons & Fractals*, vol. 23, pp. 589-600,Jan 2005.

[4] S. C. Tsay, C. K. Huang, D. L. Qiu, and W. T. Chen,"Implementation of bidirectional chaotic communication systems based on Lorenz circuits," *Chaos Solitons & Fractals*, vol. 20, pp. 567-579, May 2004.

[5] M. Itoh, "Synthesis of electronic circuits for simulating nonlinear dynamics," *International Journal of Bifurcation and Chaos*, vol. 11, pp. 605-653,Mar 2001.

[6] H. H. Chen,"Stability and chaotic dynamics of a perturbed rate gyro," *Chaos Solitons & Fractals*, vol. 30, pp. 822-835,Nov 2006.

[7] Z. Wang, and K. T. Chau,"Anti-control of chaos of a permanent magnet DC motor system for vibratory compactors," *Chaos Solitons & Fractals*, vol. 36, pp. 694-708, May 2008.

[8] C. L. Huang,"Nonlinear Dynamics of the Horizontal Platform," *Master of Science in Mechanical Engineering Thesis*,NCTU,1996.

[9] Z. M. Ge, T. C. Yu, and Y. S. Chen,"Chaos synchronization of a horizontal platform system," *Journal of Sound and Vibration*, vol. 268, pp. 731-749, Dec 2003.

[10] X. F. Wu, J. P. Cai, and M. H. Wang,"Master-slave chaos synchronization criteria for the horizontal platform systems via linear state error feedback control," *Journal of Sound and Vibration*, vol. 295, pp. 378-387,Aug 2006.

[11] X. F. Wu, J. P. Cai, and M. H. Wang,"Robust synchronization of chaotic horizontal platform systems with phase difference," *Journal of Sound and Vibration*, vol. 305, pp. 481-491,Aug 2007.

[12] J. Y. Lee,"The corresponding phenomena of mechanical and electronic impact oscillator," *Journal of Sound and Vibration*, vol. 311, pp. 579-587 ,Mar 2008.

[13] C. C. Wang, and H. T. Yau, "Analysis of nonlinear dynamic behavior of atomic force microscope using differential transformation method," *ACTA Mechanica*, vol. 198, pp. 87-98, 2008.

[14] C. C. Wang, "Application of a hybrid method to the nonlinear dynamic analysis of a spherical gas journal bearing system," *Nonlinear Analysis-Theory Methods & Applications*, vol.70, pp. 2035-2053, 2009.

[15] C. C. Wang, "Chaotic analysis and control of microcandilevers with PD feedback using differential transformation method," *International Journal of Nonlinear Sciences and Numerical Simulation*, vol. 10, pp. 425-444, April 2009.

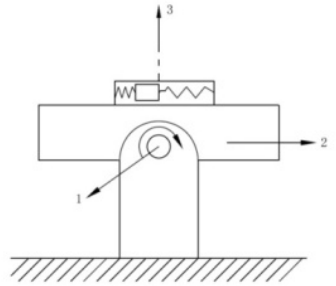

Fig. 1 The horizontal platform system.

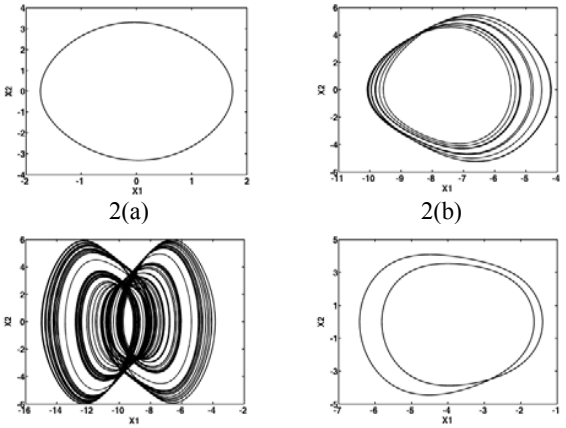

2(a) 2(b)

2(c) 2(d)

Fig. 2 Phase portraits of HPS at *F*=(a)1.33, (b)2.78, (c)3.21, (d)3.59.

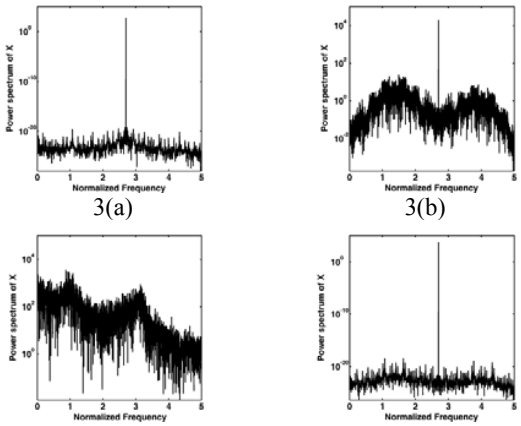

3(a) 3(b)

3(c) 3(d)

Fig. 3 Power spectra of HPS at *F*=(a)1.33, (b)2.78, (c)3.21, (d)3.59.

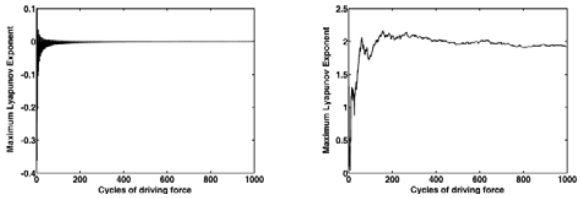

4(a) 4(b)

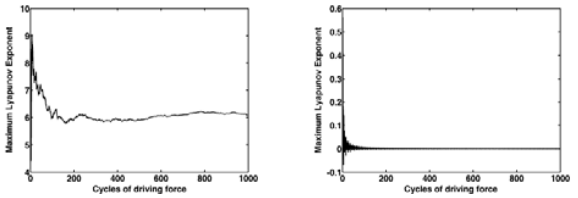

4(c) 4(d)

Fig. 4 Lyapunov exponent at F=(a)1.33, (b)2.78, (c)3.21, (d)3.59.

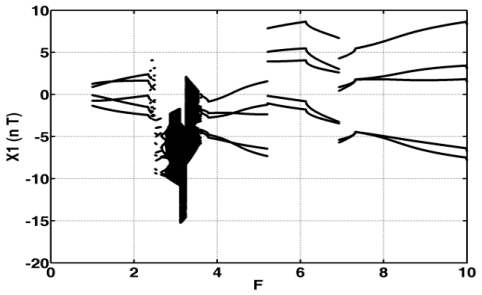

5(a)

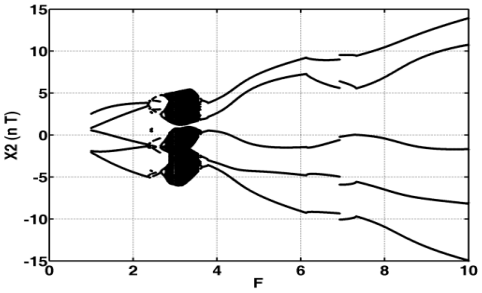

5(b)

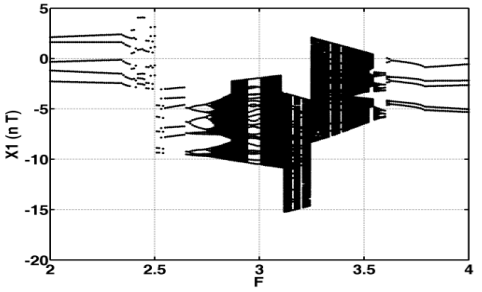

5(c)

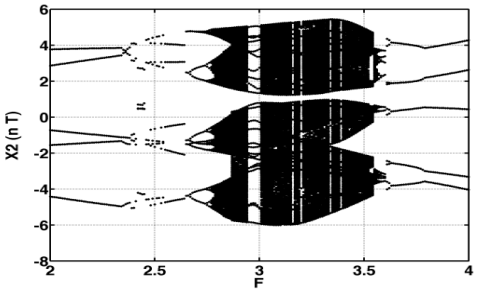

5(d)

Fig. 5 Bifurcation diagrams: (a) for X_1 (F=1~10), (b) for X_2 (F=1~10), (c) for X_1 (F=2~4), (d) for X_2 (F=2~4)

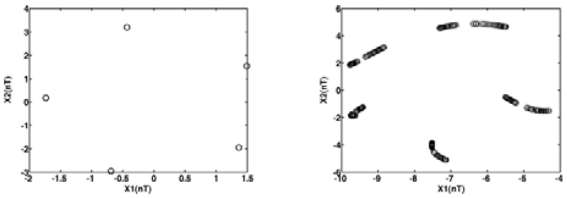

6(a) 6(b)

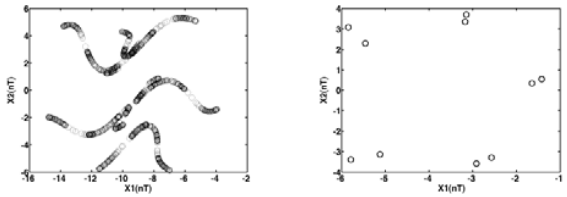

6(c) 6(d)

Fig. 6 Poincaré maps of HPS at F=(a)1.33, (b)2.78, (c)3.21, (d)3.59.

TABLE I
COMPARISON OF POINCARÉ MAPS OF HPS OBIT DATA CALCULATED BY DTM AND RKM METHODS

Displacement / Conditions		X_1(nT)		X_2(nT)	
		H (time step)			
		0.001	0.01	0.001	0.01
DTM	F = 1.33	1.22312178	1.22312689	-2.42342159	-2.42342159
RKM		1.22310511	1.22305476	-2.42311762	-2.42346771
DTM	F = 3.59	-3.21431351	-3.21435217	-3.51789121	-3.51781311
RKM		-3.21410872	-3.21438856	-3.51711441	-3.51782098

TABLE II
EVOLUTION OF ROTOR BEHAVIOR OVER ROTOR MASS INTERVAL $1 \leq F \leq 10$

F	**[1,2.67)**	**[2.67,2.75)**	**[2.75,2.78)**	**[2.78,2.95)**	**[2.95,3.0)**
Dynamic behavior	**5T**	**10T**	**Multi**	**Chaos**	**Multi**
F	**[3.01,3.2)**	**[3.2,3.21)**	**[3.21,3.34)**	**[3.34,3.35)**	**[3.35,3.39)**
Dynamic behavior	**Chaos**	**Multi**	**Chaos**	**Multi**	**Chaos**
F	**[3.39,3.4)**	**[3.40,3.57)**	**[3.57,3.59)**	**[3.59,3.63)**	**[3.63,10.0]**
Dynamic behavior	**Multi**	**Chaos**	**Multi**	**10T**	**5T**